DOE/MC/30086 -- 5510

Naturally Fractured Tight Gas - Gas Reservoir Detection Optimization

Quarterly Report
June 1 - September 30, 1996

By:
J. Miles Maxwell
Peter Ortoleva
Dorothy Payne
Walid Sibo

Work Performed Under Contract No.: DE-AC21-93MC30086

For
U.S. Department of Energy
Office of Fossil Energy
Federal Energy Technology Center
Morgantown Site
P.O. Box 880
Morgantown, West Virginia 26507-0880

DISTRIBUTION OF THIS DOCUMENT IS UNLIMITED

By
Advanced Resources International, Inc.
165 South Union Boulevard
Suite 800
Denver, Colorado 80228

MASTER

Disclaimer

This report was prepared as an account of work sponsored by an agency of the United States Government. Neither the United States Government nor any agency thereof, nor any of their employees, makes any warranty, express or implied, or assumes any legal liability or responsibility for the accuracy, completeness, or usefulness of any information, apparatus, product, or process disclosed, or represents that its use would not infringe privately owned rights. Reference herein to any specific commercial product, process, or service by trade name, trademark, manufacturer, or otherwise does not necessarily constitute or imply its endorsement, recommendation, or favoring by the United States Government or any agency thereof. The views and opinions of authors expressed herein do not necessarily state or reflect those of the United States Government or any agency thereof.

DISCLAIMER

Portions of this document may be illegible electronic image products. Images are produced from the best available original document.

QUARTERLY STATUS REPORT
Period of Performance: June 1 - September 30, 1996
Date of Submission: November 15, 1996

CONTRACT NO.

DE-AC21-93MC30086

CONTRACTOR:

Advanced Resources International, Inc.
165 South Union Boulevard, Suite 800
Denver, Colorado 80228

CONTRACT NAME:

Naturally Fractured Tight Gas
Gas Reservoir Detection
Optimization

CONTRACT PERIOD:

09/30/93 - 03/31/97

RECEIVED
NOV 10 1997
OSTI

CONTRACT OBJECTIVE: No Change

TECHNICAL APPROACH CHANGES: No Change

RULISON 3-D P-WAVE DATA PROCESSING:

The processing of the 3-D P-wave data was conducted at Western Geophysical. Refraction statics were calculated. Normal moveout velocities for the all-azimuth volume were determined from vel-scans. The data were stacked using the new, improved statics and normal moveout velocities. Good signal/ noise are observed from above target to Dakota Sandstone (2.5 sec, well below target at 1.3 - 1.5 sec). The data show fairly flat-lying reflectors with some possible faulting or stratigraphic variation in the Cameo Coal sequence.

The initial azimuth bin gathers were constructed and sent to H.B. Lynn. The velocities for the initial bin gathers were instrumental to reveal the azimuthal variation in velocity and amplitude and AVO (amplitude variation w/ effect). The five azimuth bin gathers at the five wells reveal that P-wave azimuthal anistropy is present at Rulison Field, thus validating the selection of Rulison as an appropriate location for the seismic 3-D project. The fast direction (P-wave) has been chosen as N150°E, based upon the azimuth bin gather data. The slow direction (P-wave) is N60°E. These two directions are interpreted as parallel and perpendicular to the open gas-filled fractures, respectively.

The 3-D data will be divided into two volumes (N150°E +/- 45° and N60°E +/- 45°) and then sent through NMO-stack-time migration for structural imaging of the reflectors.

The four azimuth volumes prepared were: N150°E +/- 22.5°, N60°E +/- 22.5°, N105°E +/- 22.5°, N15°E +/- 22.5°. These data volumes are the input to the Western Geophysical "Fractogram" program, which evaluates the change of amplitude with offset and azimuth.

Data tapes were shipped from Western Geophysical to Lynn, Inc., for interpretation. The data tapes included wiggle trace data (post-stack time migration seismic data) and velocity data (stacking velocity cubes).

The two-azimuth volumes are source-receivers in the "fast" P-wave velocity direction, N150E (N30W), and the "slow" P-wave velocity direction (N60E). Spatial variability in the direction of the "fast" P-wave, and spacial variability in the magnitude of the difference of the two velocities, are observed in the Rulison 3-D dataset. Velocity cubes for each azimuth have also been used for determining interval velocities associated with the two different azimuths.

The seismic attribute that best approximates the Estimated Ultimate Recovery is the ratio of the interval velocities in the gas-saturated Mesaverde interval (the "Z" reflector to the top of Cameo Coal reflector). This result is consistent with the findings of the other DOE/Morgantown project, in the Madden Field, Wind River, WY: the ratio of the interval velocities (perpendicular to the fractures, or the slow direction, divided by the parallel to fractures directions, that is, the fast direction) showed the best correlation to the EUR, as furnished by a population of 12 wells.

We have also examined the reflection amplitude data and have determined that there appears to be a near-surface effect which is present on all reflectors and in all interval amplitude measurements down to the Corcoran (about 1.5 sec. below the target zone). This near-surface effect appears to be caused by an anisotropic weathering layer, which is affecting the quality of transmission of reflection signal, dependent upon azimuth of source-receiver. Therefore, we are devising techniques, acceptable to industry conventional standards, to deal with this problem. The consequence of this near-surface effect is that AVO (amplitude variation with offset) analysis and reflection strength analysis cannot be accomplished until this problem is solved.

3-D BASIN MODELING:

The 3-D Basin modeling effort is continuing with code development. Focus of the modeling is pressure, porosity and permeability development that occurs during early diagnostic sedimentary compaction and dewatering phase. The profound influence of gas generation during catagenesis, several periods of uplift, erosion and laramide compression and thrusting on fracture development are scheduled for future modeling.

A data base of 56 pressure build-up tests from short-term drill-stem tests (DST's) were used to generate 3-D pressure gradient maps. Due to low matrix permeability, the short build up times of DST's are inadequate to measure actual reservoir pressure. As such, the pressure data severely underestimates true reservoir pressure and the resulting pressure gradient map is dominated by an underpressured regime with an occasional patch of over pressure. The pressure gradient map is not consistent with previously published pressure gradient maps and does not honor accurate pressure data supplied by ARI. This discrepancy has been raised in the past with no acknowledgment or modifications from the subcontractor.

The highly compartmentalized basin interpretation derived from the erroneous pressure gradient map is roughly symmetrical with compartmentalization predicted during early diagnosis (70 million years ago) and is viewed as model validation. This conclusion ignores that the present-day basis is gas

filled as opposed to the early water filled, diagentic basin. The subcontractor has scheduled national and regional presentation of project results during October and November. There has been no response to ARI's requesting that all presentation material be forwarded for review and approval according to DOE/METC requirements.

A six-month plan for completing the basin modeling by March, 1997 has been received. A review of project results and 1997 work plan has been scheduled at subcontractor's facilities in Bloomington, Indiana during early December. The contractor's detailed quarterly report is included as an attachment.

OPEN ITEMS: None

David Decker

Attachment: Laboratory for Computational Geochemistry Quarterly Report

Summary

The main activities of this quarter were

- analysis of the fluid pressure data to understand the compartment structure of the basin and for use as a verification of our basin simulator/fractured reservoir predictor;
- develop an improved sedimentary history/lithologic unit geometry reconstruction algorithm and computer module; and
- further improvement, verification and debugging of the basin stress and multi-phase reaction-transport module.

The first two elements are described in more detail in the following sections.

Completion of the code development/verification for the mechanical and multi-phase modules should be done by next quarter. Delays in code development are due to the unforeseen difficulties caused by the budget reduction from that originally proposed.

Contents

I Pressure Data: Analysis and Delineation of Compartments

In this section, we review the available pressure data and its implications for the location and characteristics of abnormal pressuring in the Piceance Basin. We conclude that abnormal pressuring and related compartmentation is in the form of a mosaic of over- and underpressured zones.

Fig. 1(a) shows the locations of pressure data points in three dimensions used to show the observed distribution of fluid pressures in the Piceance Basin and to calibrate the model; Fig. 1(b) shows a map view of the interpolation grid with latitude and longitude values along the axes. Fifty-six highest quality data points from thirty-one wells were taken from a list of pressure data compiled by the Texas Bureau of Economic Geology (TBEG). In this data set, shut-in times of drill stem tests (DSTs) were used to distinguish data groups of varying confidence levels: high quality data refers to data from DSTs in which shut-in times were greater than one hour; the remainder of the data was classified as moderate quality if the shut-in times were 30 to 60 minutes, or unknown if this information was unavailable (Kaiser and Scott, 1996). In Fig. 1(a), these data points represent the subset of data in which there is the greatest confidence. Most of the data locations, forty-six points, are within the Mesaverde Group, seven are in the overlying Tertiary units, and three are in the Mancos or older groups. The actual pressure values range from 682 psi (about 47 bars) to 5462 psi (about 376 bars). Overpressuring, defined as the fluid pressure minus hydrostatic pressure, ranges from -103 bars to 56 bars.

Using our data interpolation package, this pressure data implies a patchy distribution of fluid pressures. Fig. 2 shows the isosurfaces of overpressure of one bar (a) and 10 bars (b). The greatest concentration of overpressure patches is in the region southeast of the central part of the basin, with fewer in the south central area and north central area. Fig. 2(c) shows the isosurfaces of -7 bars underpressure. Underpressure

appears as a cluster of patches in the southern part of the basin, as well as a large continuous area in the northern part of the basin. Most of the smaller patches in the southern part of the basin are interspersed with the overpressure patches. In some cases the overpressure zone resides within an underpressured patch. Thus, in these regions overpressuring and underpressuring alternate in a vertical sequence. Likewise, the larger surface of underpressuring in the north encloses smaller patches of overpressuring located there.

This mosaic character may be illustrated by examining the overpressure distribution on isochron surfaces. Figs. 3(c-f) show map views of pressure distribution on isochrons between the 70.1 mya isochron (Fig. 3(a)) and the 72.6 mya isochron (Fig. 3(b)). Figs. 3(c-e) show three small, isolated overpressure compartments: the 70.2 mya isochron, the 70.35 mya isochron, and the 72.6 mya isochron. These overpressure compartments are enclosed within and separated by the ambient underpressure. Fig. 3(f) shows distinct strongly underpressured and normally pressured compartments, enclosed within the ambient underpressure (approximately -10 bars) on the 71.0 mya isochron. In addition, a diffuse zone of underpressure exists in the north central part of the basin, one of the deeper parts of the basin, just west of the deepest part of the basin. This is contrary to intuition, as it might be expected that deeper parts of the basin should tend to exhibit greater fluid pressures because of thermal expansion of fluids and compaction. This figure suggests that the hydrologic system of the Piceance Basin is rather complex.

We believe that the patches of overpressure and underpressure will correlate with structures in the Wolf Creek and Divide Creek Anticlines, as well as block faulting in the Rulison Field area, and structures in the Piceance Creek and Sulphur Creek areas in the northern part of the basin (Fig. 4). This correlation may be the result of their location in or proximity to fields, which usually are developed around major structures, or may reflect a structural control on fluid pressure distribution in the basin. In the next quarter, we will examine the nature of this correlation in more detail.

The patchy nature of the fluid pressure distribution is not surprising in light of the heterogeneity of the reservoirs and their tight, largely fractured-controlled permeability. Some caution is advised, however, because of the low data density. For example, it is possible that overpressure occurs in a continuous zone of sinuously connected domains, the sinuous connections being missed by the low data density. The lithologic variability of the Mesaverde Group, especially the non-marine units of the Williams Fork Formation and overlying strata, is highly variable, comprising interbedded mudstones and fine grained fluvial channel sandstones, with interspersed coaly deposits. This results in units of complex morphology that are laterally discontinuous and not easily predictable in their subsurface location. Possible sinuous connections between overpressure zones could be through fluvial channel sandstones, although we don't have sufficient data yet to test this conjecture. In addition, the grain size and composition are variable, resulting in typically low permeability sandstones. Permeability and porosity are believed to be largely fracture controlled. Thus, the abnormal fluid pressure distribution will be largely influenced by the geometry, connectivity, and extent of the fracture network system.

These figures suggest that the Piceance reservoir system is highly compartmentalized. A study of the hydrology of the Piceance Basin by the TBEG (Kaiser and Scott, 1996), in which the above mentioned pressure data was used, supports this. They show that it is an unintegrated flow system, divided by permeability contrasts, faults and facies changes, as well as abnormal pressure zones. Thus, even with a greater density distribution of reliable data, we believe the resulting pressure distribution will have the same mosaic character, as shown in the above figures. Figs. 5(a-d) shows the distribution of pressure using an additional 75 points from the TBEG data set, although the confidence in this additional data, as evaluated by TBEG, is lower.

For comparison, we illustrate the distribution of abnormal pressures and compartmentation in the Anadarko Basin. Fig. 6(a) shows the distribution of points for which quality-screened pressure data was available. The quality analysis of this data was

performed by Al-Shaieb and co-workers at Oklahoma State University. As determined by data points in Fig. 6(a) and our interpolation scheme, Figs. 6(b-d) show isosurfaces of underpressure and overpressure in the Anadarko Basin. In the Anadarko Basin, there are larger, more continuous regions of abnormal pressure, with significant overpressuring predominant in the south central part of the basin, and underpressuring in the northwestern half of the basin and toward the deep eastern margin of the basin. These figures suggest the presence of large abnormal pressure compartments in the basin, as well as clusters of smaller compartments lying outside the larger compartments. The differences in the character of pressure compartments in the Anadarko Basin relative to that of the Piceance Basin may be attributed to two factors, a geologic factor and a data density factor. First, the Anadarko Basin contains lithologies with more conventional intergranular porosity and permeability, which allows much greater fluid communication across larger areas of the basin. This is in contrast to the hydrologically unintegrated Piceance Basin. Secondly, over 2900 pressure data values were used in the Anadarko Basin, allowing a much better resolution of the pressure distribution. This is in contrast to fewer than 200 data points in the above Piceance Basin study.

It is important to note that data availability and selection will affect the interpreted three dimensional character of the fluid pressure distribution. For example, Fig. 7 shows the 10 bar overpressure isosurface using only the normal to overpressure values of the high quality TBEG data set. In other words, the high quality data set has been arbitrarily screened by removing all underpressure values, leaving only 16 pressure data points in the normal to overpressure range. In contrast to Fig. 2(b), this isosurface is large and continuous in nature, and does not show the mosaic character. In selecting the data in this way, the fluid pressure profile resembles more closely what is expected to be the compartment style of basins with more conventional intergranular porosity and permeability. From this, we conclude that it may be dangerous to simply extrapolate one's view from experience in other basins by neglecting data inconsistent with this view.

II Sedimentary History Reconstruction Module

A final improvement in the sedimentary history reconstruction module has been developed and will be implemented by the end of October 1996. As earlier the data input is in the form of well files. These files contain petrologic and age data at a set of well locations. The output of this module is the rate and texture of sediments laid down at any point in the basin at any specified time during the evolution of the basin.

In our earlier approach, the interwell interpolation formulae had the problem that contacts between lithologies were often artificially jagged, although the approach did preserve sharp changes of texture across contacts. In the new approach, the contact irregularity problem is alleviated by dividing the map into a set of triangles whose vertices lie at the well sites. Then the shape of a contact can be constructed geometrically within each triangle so as to be continuous across the basin.

A key to our practical implementation of this approach is to automatically create the triangular subdivision of the map by a computational algorithm. An example of such a computer generated subdivision of our Piceance Basin simulation domain is seen in Fig. 6.

There are several special cases for the sedimentary history reconstruction at a point in map view of the basin:

- the point lies outside the triangulated region (see Fig. 6); or
- the point lies within a triangle with three vertices such that
  - (a) all vertices (wells) have the same lithology;
  - (b) one vertex is a different lithology from the other two; or
  - (c) all three vertices are different lithologies.

We believe that the result is the only sedimentary history reconstruction module that

- preserves sharp contrasts of texture across lithologic boundaries, and
- integrates space and time data to predict the morphologies of sedimentary bodies in three dimensions.

Next quarter, we shall include a detailed examination of the key formations in the Piceance Basin and of the entire sediment package using our new reconstruction algorithm. This shall be invaluable in exploration and development projects in general, and for naturally fractured reservoir prediction in particular. In the latter context, the mechanical properties of various lithologies enter into the computation of stress. Hence, an accurate characterization of the geometry and texture of these lithologies is a central issue.

III Preliminary Piceance Basin Simulations

Simulations of the Piceance Basin using the CIRF.B three dimensional simulator are being run. Initial runs use a simplified quartz and water chemistry, constant grain size, and simplified burial and thermal histories. The three dimensional domain is as in Figs. 1-3, and it captures the shape of the basin as determined from our 42 well sediment history reconstruction data set (see earlier quarterly reports for further detail on this data set).

Preliminary results show that grain size affects the development of fluid pressure compartments and hydro-fracturing. Figs. 9(a-b) are cross sections through the three-dimensional simulation domain, along an east-west transect in the central part of the basin (Fig. 1(b)). Generally, finer-grained systems are more likely to develop abnormal pressure compartments and fracturing (Fig. 9(b)). Furthermore, because of their higher matrix permeability, coarser-grained systems may also develop abnormal pressures, but the pressure gradients are not as steep, making the boundaries between fluid pressure regimes more diffuse (Fig. 9(a)). It is interesting to note that even without grain size variation (i.e. sedimentary features imposed at deposition), overpressuring may develop a patchy distribution, as shown in Fig. 9(b). With more detailed accounting of sedimentary features specific to the Piceance Basin, we believe that the model will predict an even more irregular distribution of abnormal pressures, like that demonstrated in the TBEG data set and Figs. 2 and 5.

Fig. 9(b) also shows that in a system bearing fine silt-sized grains such as this simulation, significant permeability may be created as a result of hydro-fracturing. The greatest permeability appears to correlate well with the largest fracture radius. This is significant as permeability and porosity in the Upper Cretaceous units of the Piceance Basin are believed to be fracture controlled.

During the next quarter, work will proceed on making the simulations more realistic by constraining the input with more complete lithologic, burial rate and thermal history data, as developed earlier during this project.

IV Work Plan for Last Six Months of Project

1. October 1996

a. Complete sedimentary history reconstruction module improvements based on new triangulation approach.

b. Complete testing of stress solver.

c. Review pressure data and its 3-d mapping for model calibration and testing.

d. Make Piceance Basin simulations.

e. Debug and optimize multi-phase reaction-transport module.

f. Complete yearly report.

g. Present results in two lectures at AAPG special workshop on basin compartments.

2. November 1996

a. Carry out Piceance Basin simulations for one aqueous phase..

b. Preliminary Piceance Basin simulations with multi-fluid phase dynamics (including methane genesis).

c. Develop data on deposited organics in the Piceance Basin

d. Present lecture at Gas Research Institute conference on compartments, contrasting examples from the Piceance Basin as compared to the Anadarko Basin.

3. December 1996

a. Simulations of Piceance Basin to predict fractured reservoir locations and characteristics and identify factors on basin history affecting them.

b. Host Advanced Resources International/Department of Energy Site visit.

c. Quarterly report preparation.

d. Edit manuscripts on fractured reservoir predictions for Piceance Basin.

4. January 1997

a. Further Piceance simulations

b. Comparison of modeling predictions with observations (in close collaboration with Advanced Resources International personnel).

5. February 1997

a. Complete manuscript on fractured reservoir predictive modeling approach.

b. Complete manuscript on detailed comparison of modeling and observations (in collaboration with Advanced Resources International personnel).

c. Start final report.

6. March 1997

a. Complete final report.

b. Prepare materials for presentations and commercial booth at 1997 Annual AAPG.

c. Formulate plans for commercialization and future applications and model development.

d. Miscellaneous issues of project completion.

References

Kaiser, W.R. and A.R. Scott (1996) Hydrologic setting of the Williams Fork Formation, Piceance Basin, Colorado, in Geologic and Hydrologic Controls Critical to Coalbed Methane Producibility and Resource Assessment: Williams Fork Formation, Piceance Basin, Northwest Colorado, GRI Topical Report, GRI-95/0532.

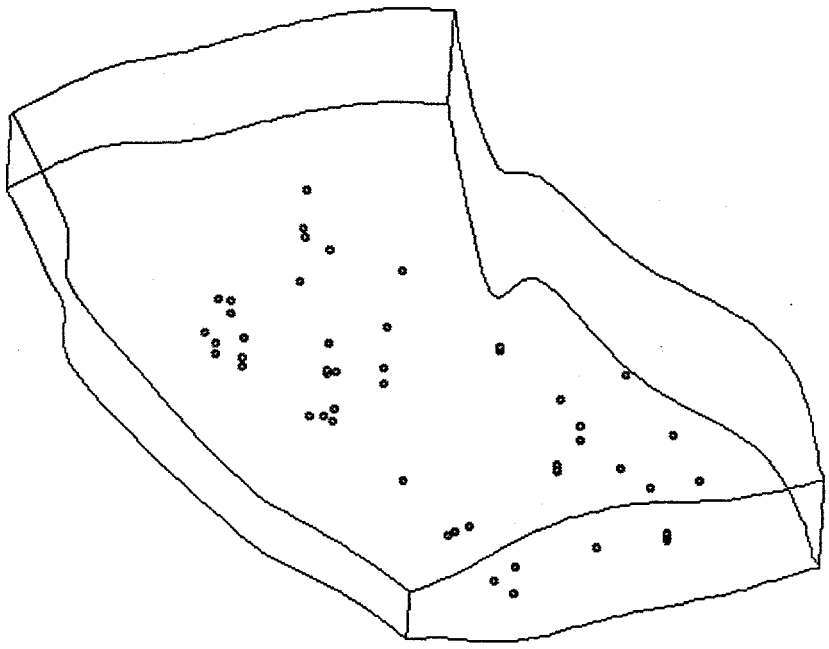

Fig. 1(a) Location of 56 high quality pressure data points, as evaluated by TBEG, in the Piceance Basin. Vertical exaggeration is 20x.

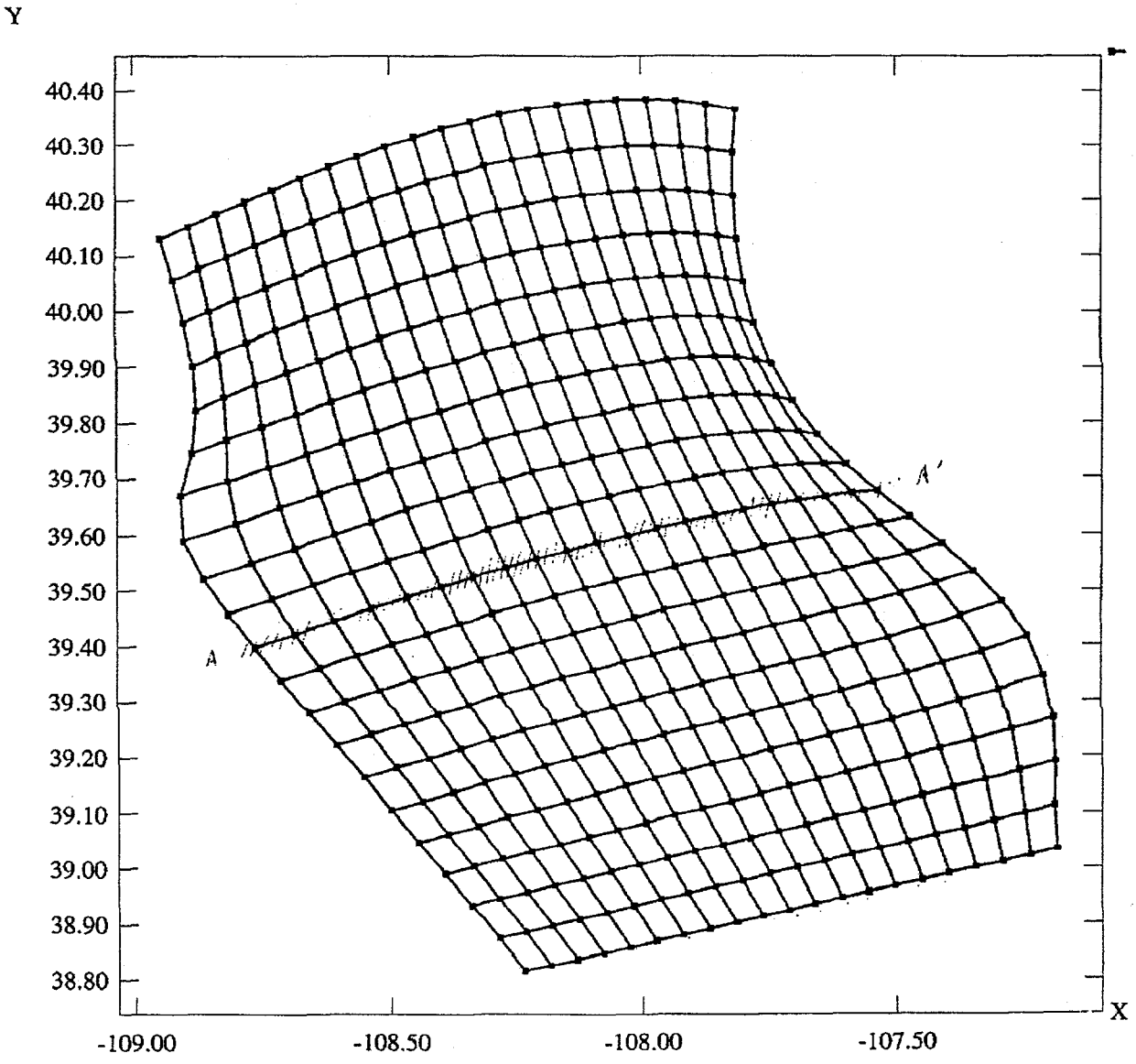

Fig. 1(b) Map view of the interpolation grid, with longitude and latitude values along the x and y axes; A-A' is location of cross-section illustrated for results of preliminary 3-D simulations.

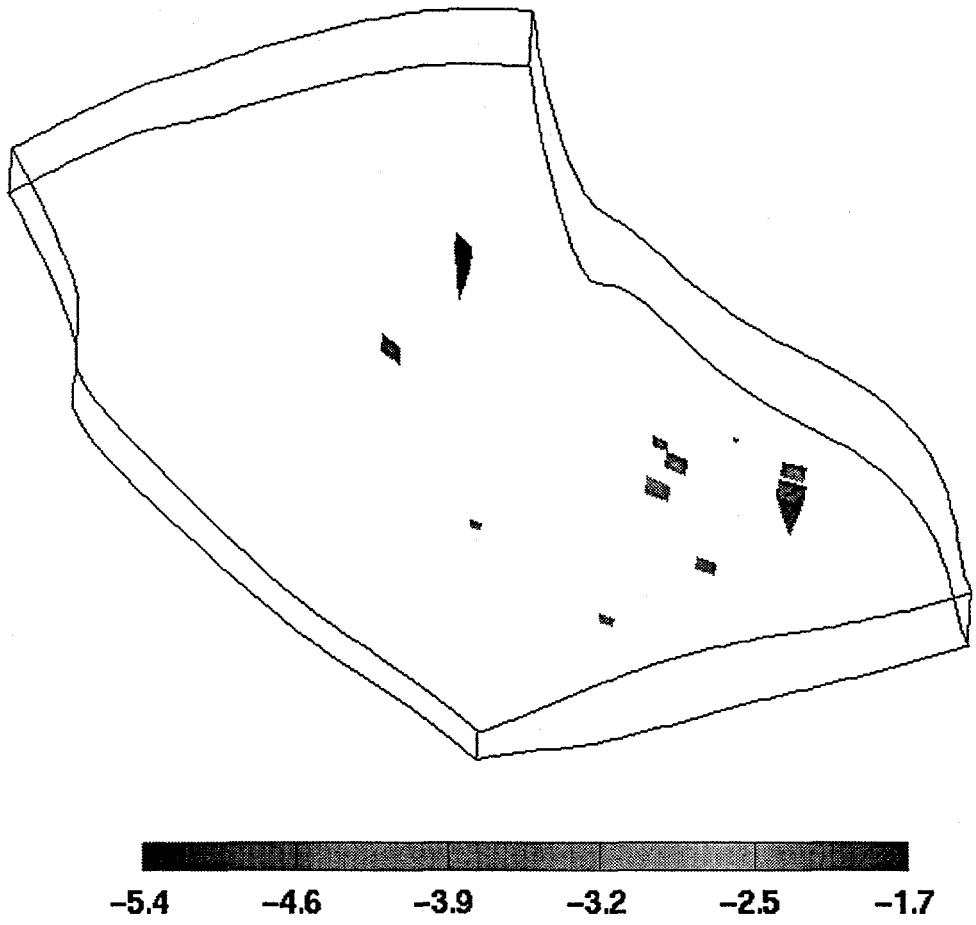

Fig. 2(a) Isosurface of 1 bar overpressure in the Piceance Basin, using highest quality pressure data; vertical exaggeration is 10x.

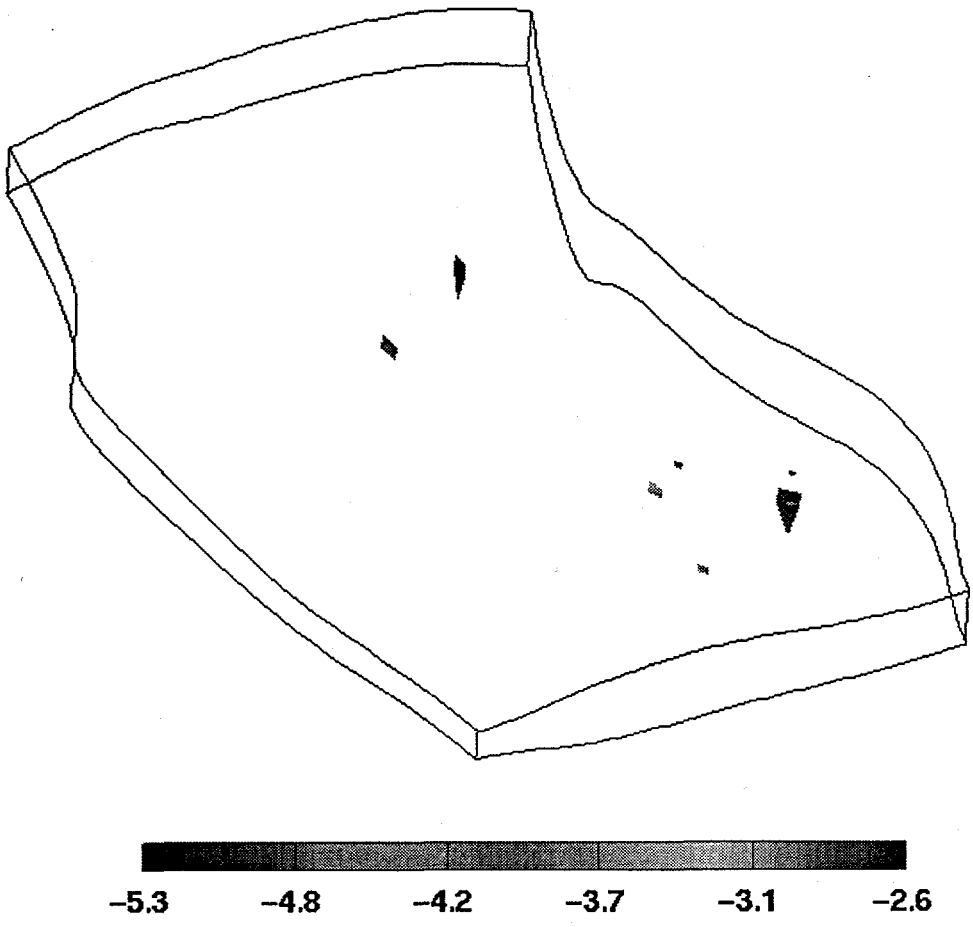

Fig. 2(b) Isosurface of 10 bars overpressure.

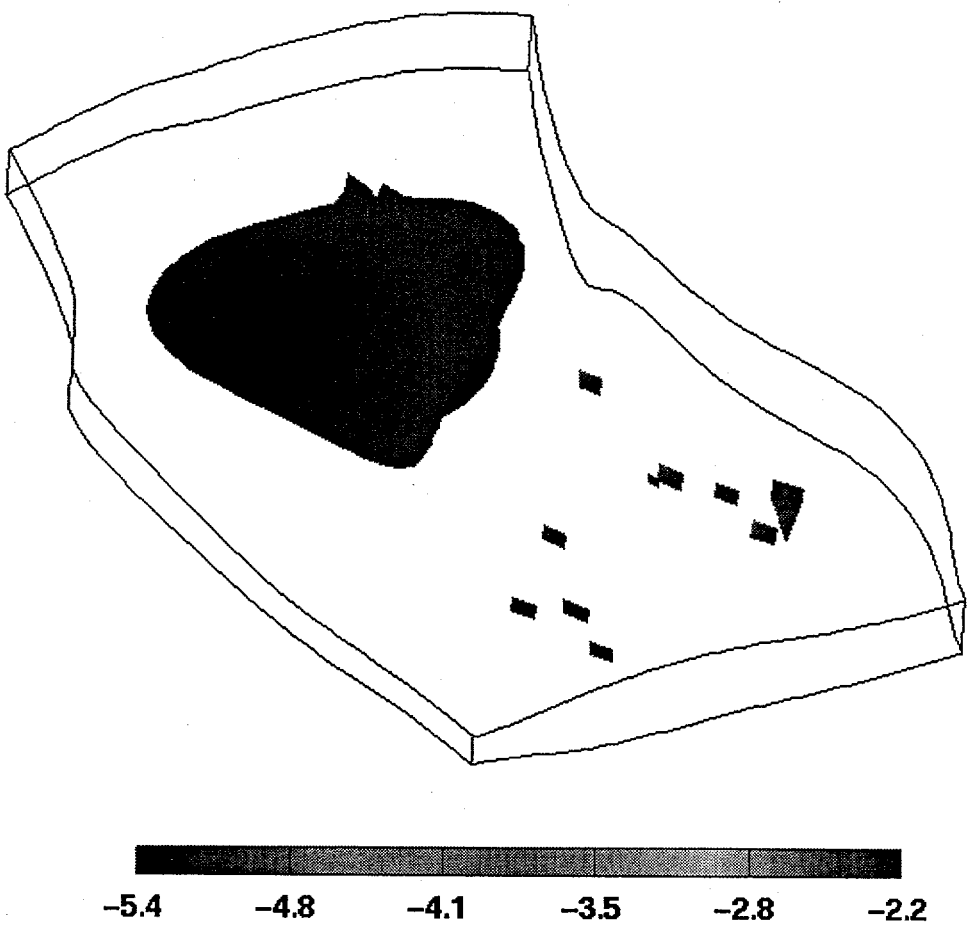

Fig. 2(c) Isosurface of 7 bars underpressure.

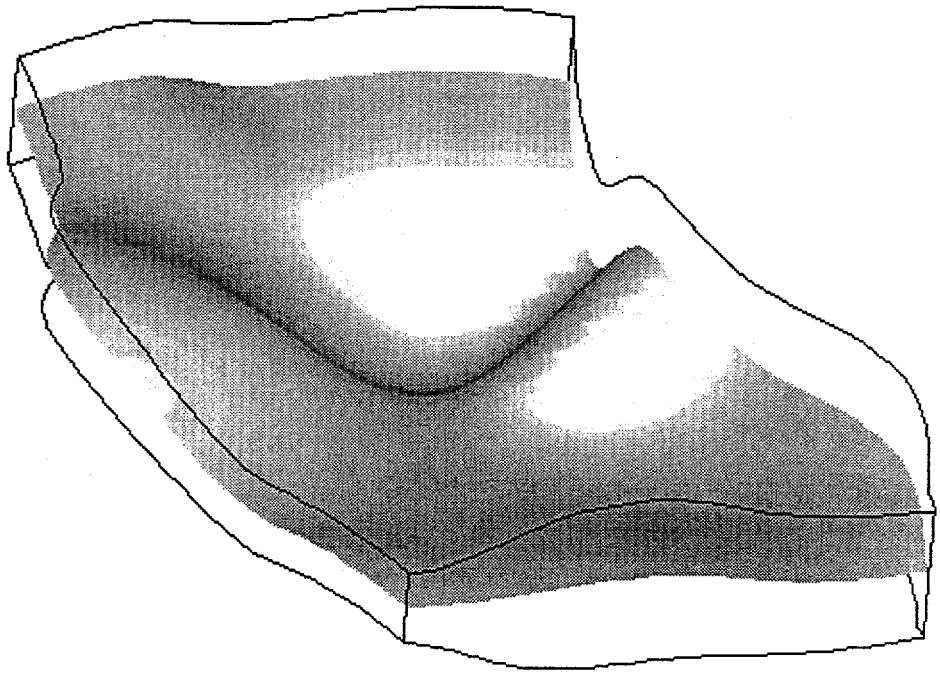

Fig. 3(a) 70.1 my isochron.

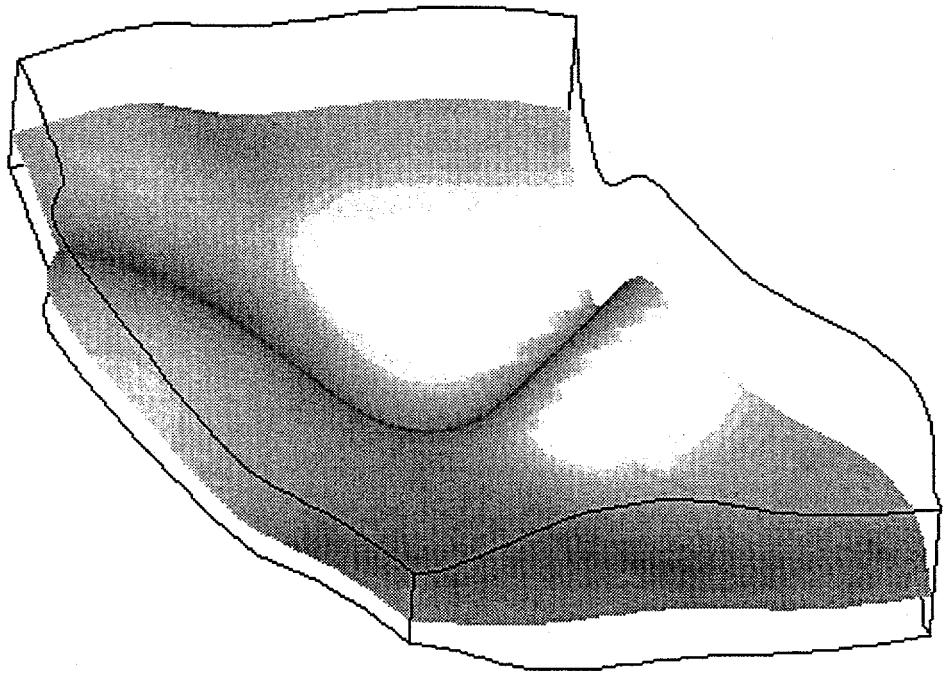

Fig. 3(b) 72.6 my isochron.

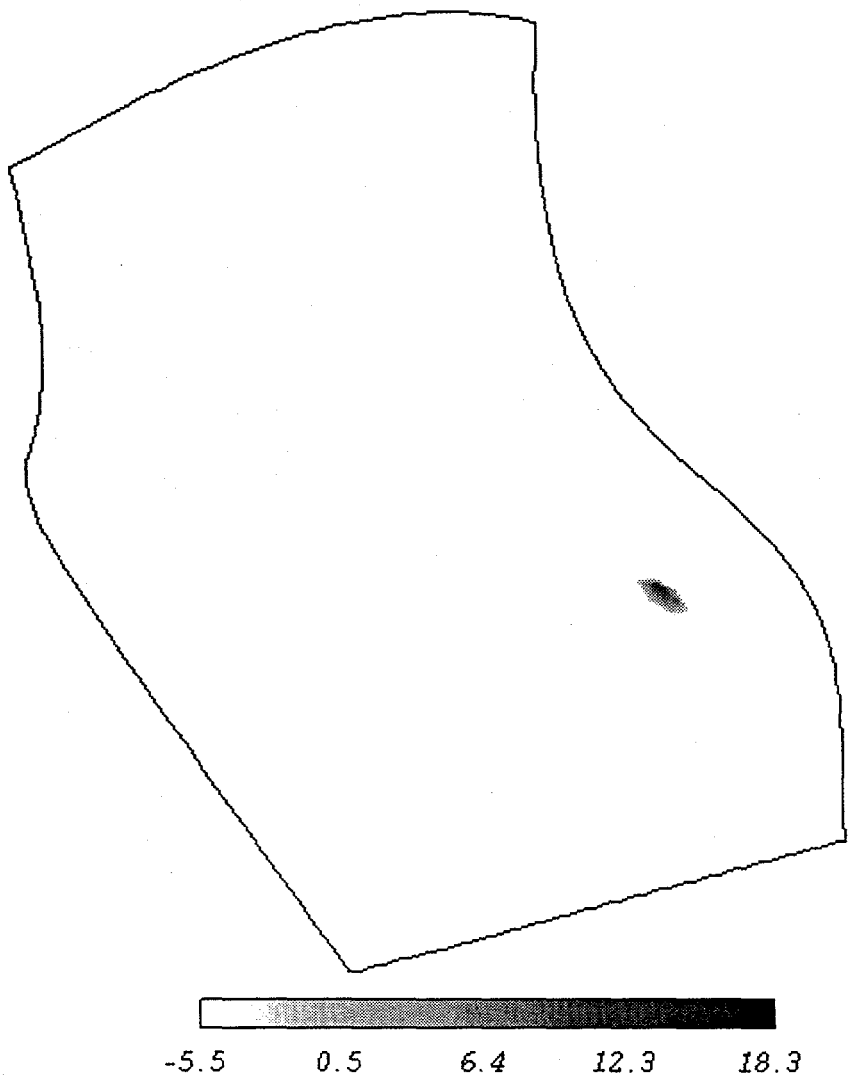

Fig. 3(c) Abnormal pressure distribution on the 70.2 my isochron.

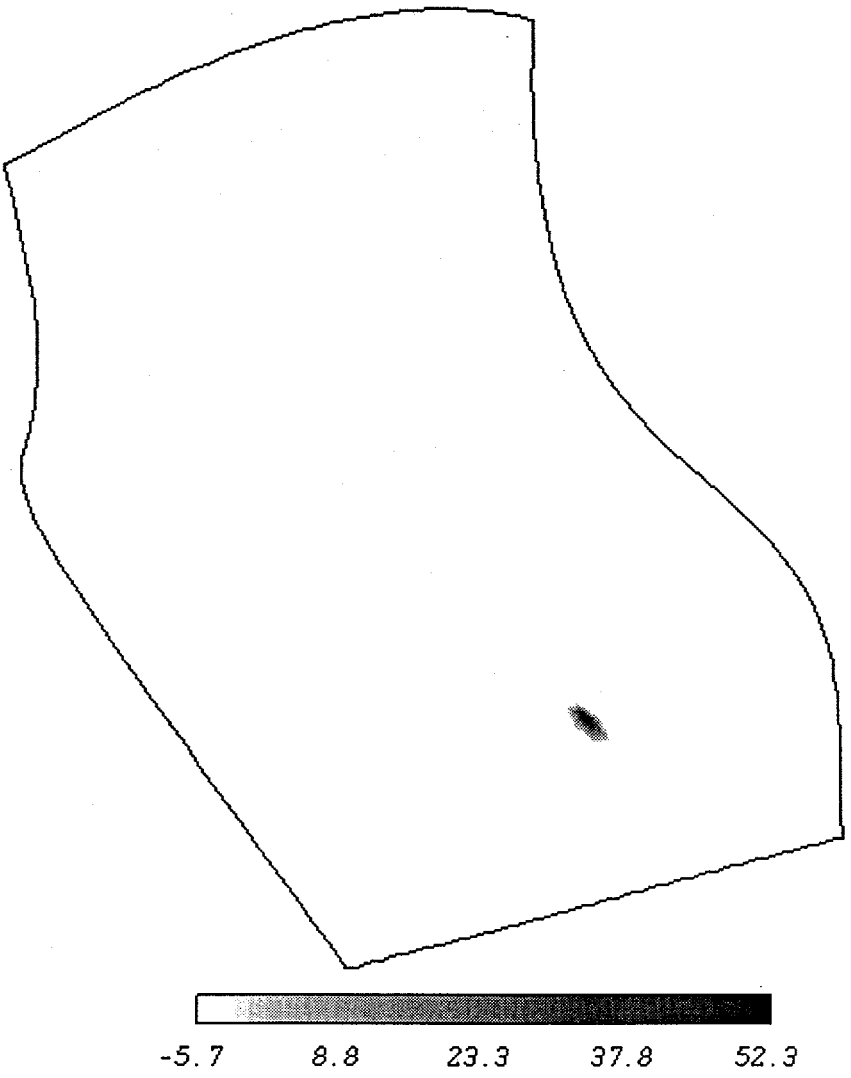

Fig. 3(d) Abnormal pressure distribution on the 70.35 my isochron.

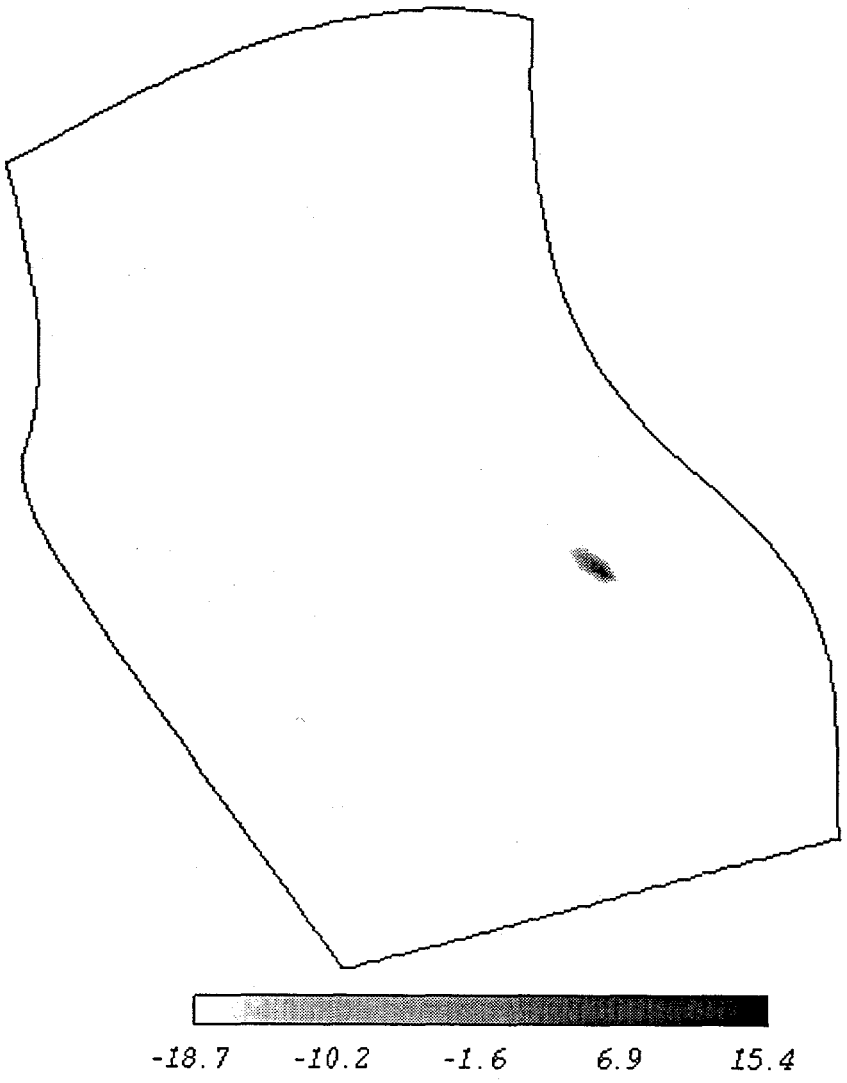

Fig. 3(e) Abnormal pressure distribution on the 72.6 my isochron.

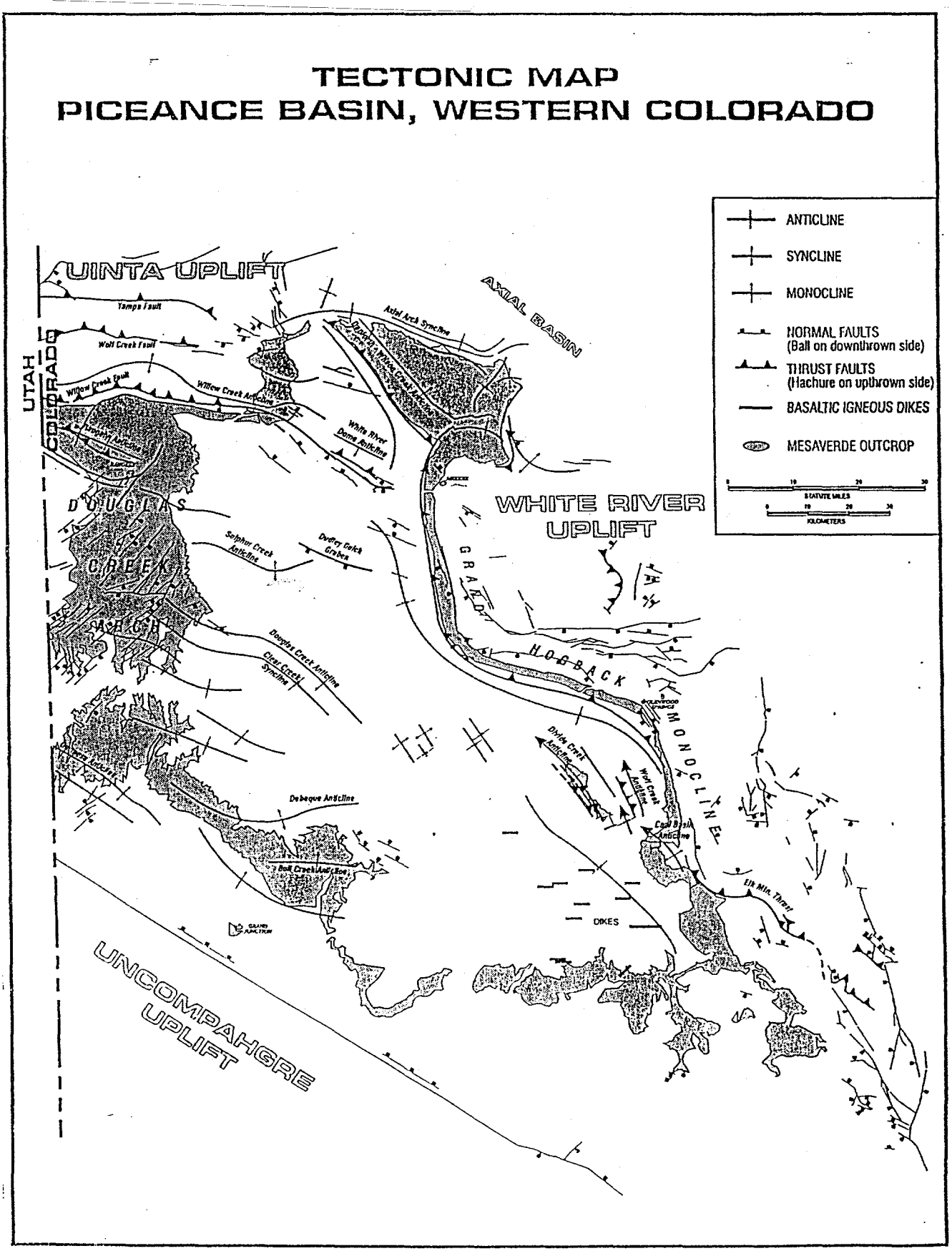

Fig. 4 Locations and types of major structures in the Piceance Basin.

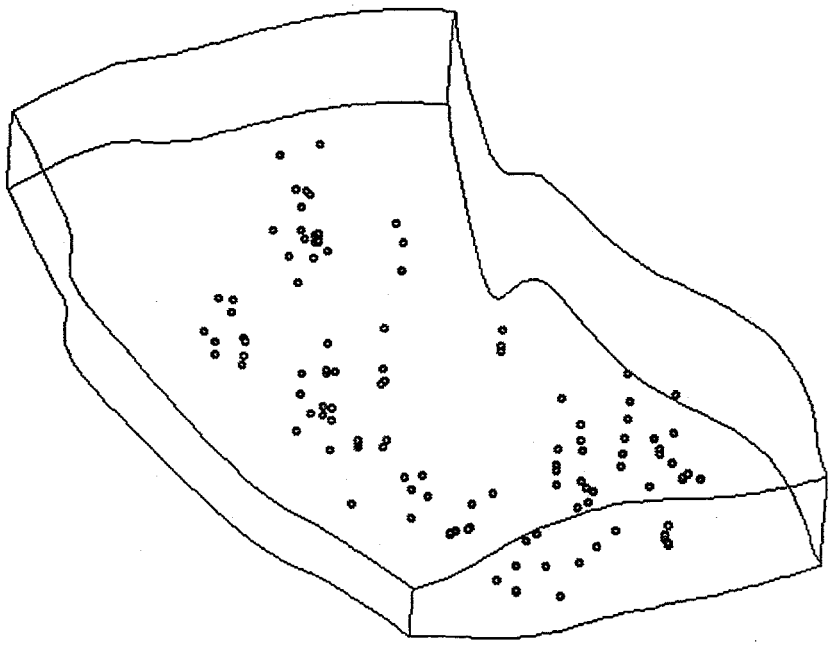

Fig. 5(a) Location of all 129 pressure data points (TBEG) in the Piceance Basin. Vertical exaggeration is 20x.

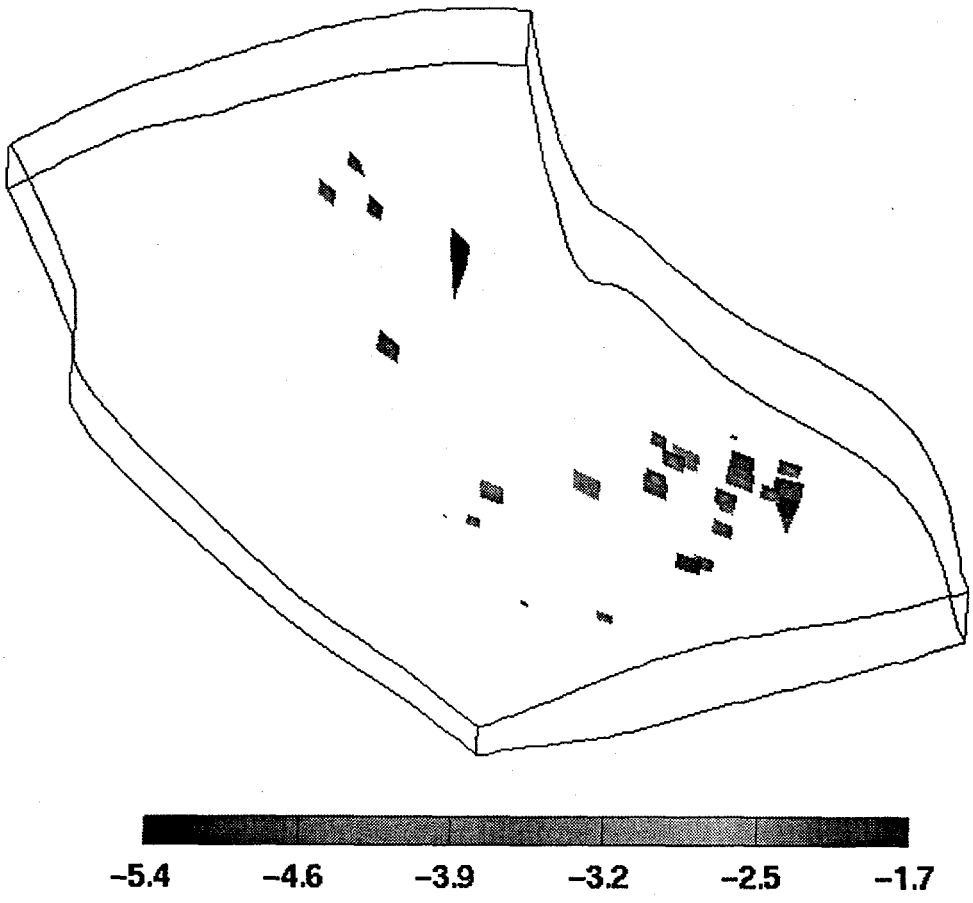

Fig. 5(b) Isosurface of 1 bar overpressure in the Piceance Basin, using high, moderate, and unknown quality data. Vertical exaggeration is 10x.

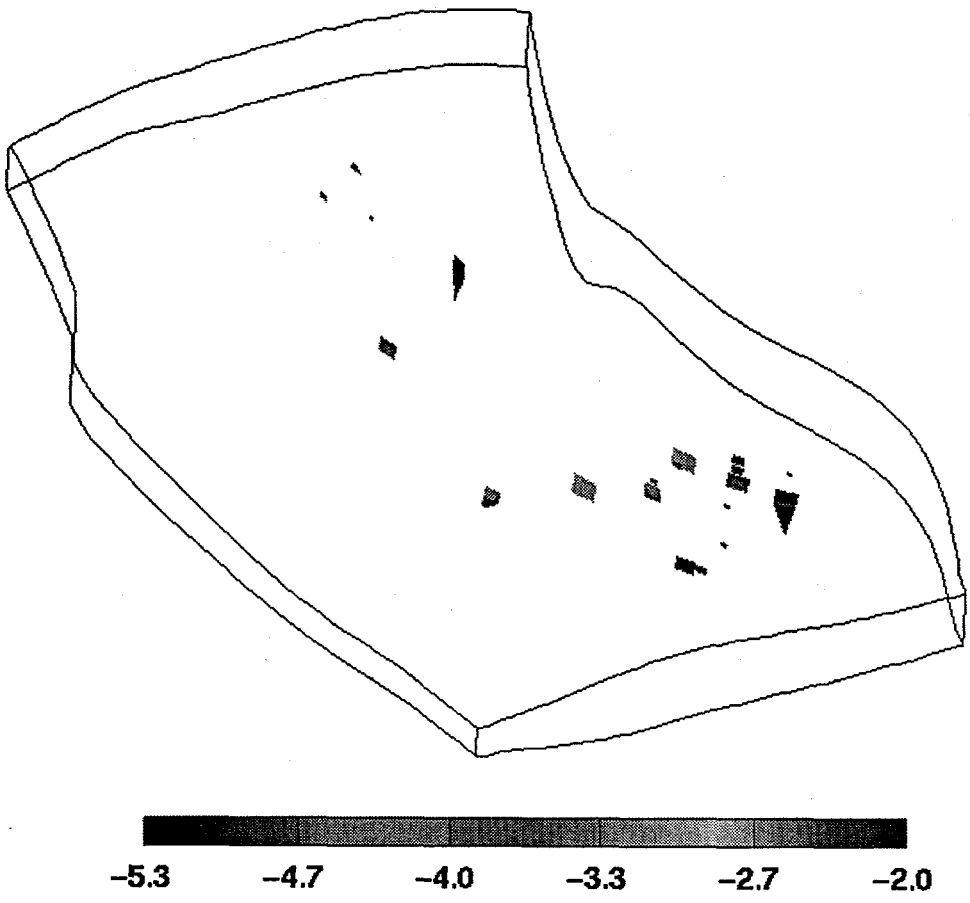

Fig. 5(c) Isosurface of 10 bars overpressure.

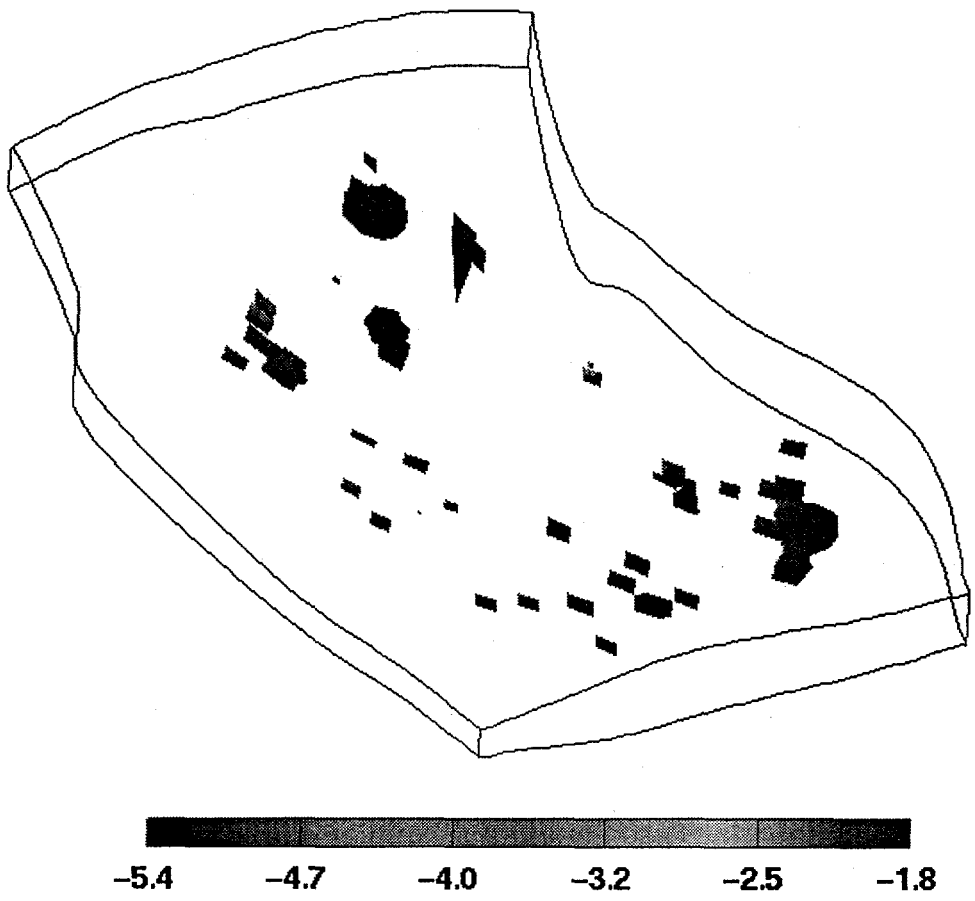

Fig. 5(d) Isosurface of 7 bars underpressure.

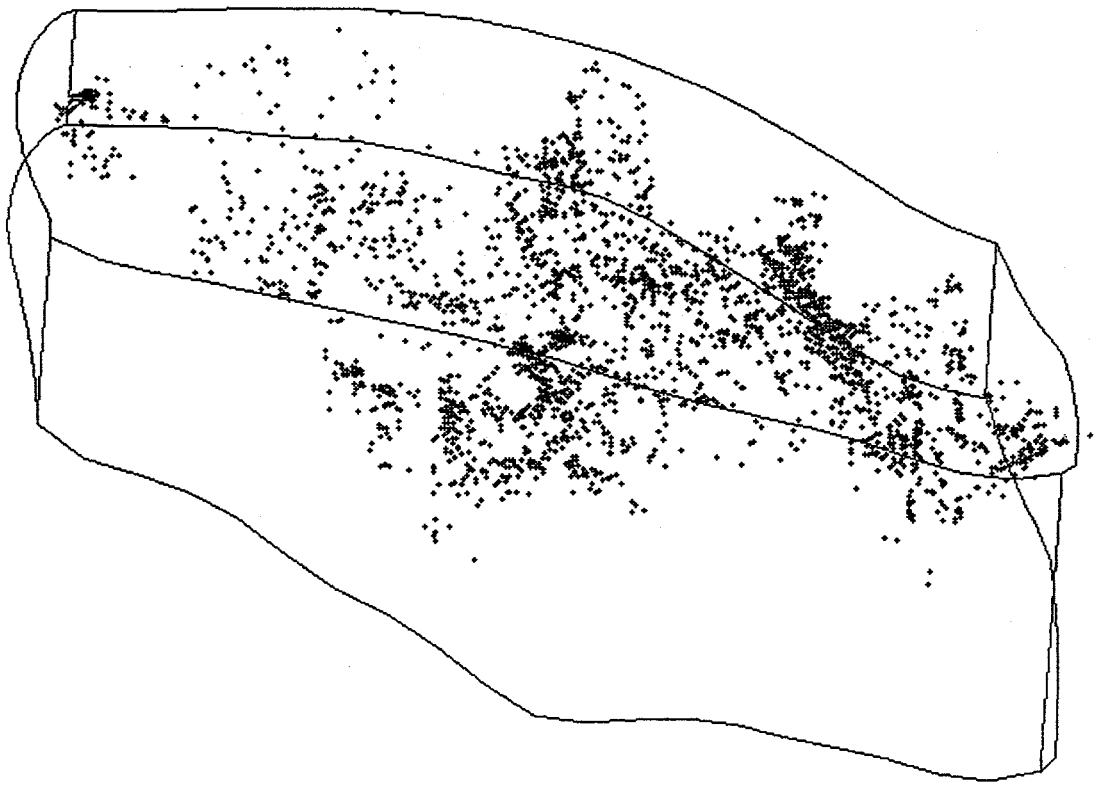

Fig. 6(a) Location of over 2900 pressure data points in the Anadarko Basin. Vertical exaggeration is 20x.

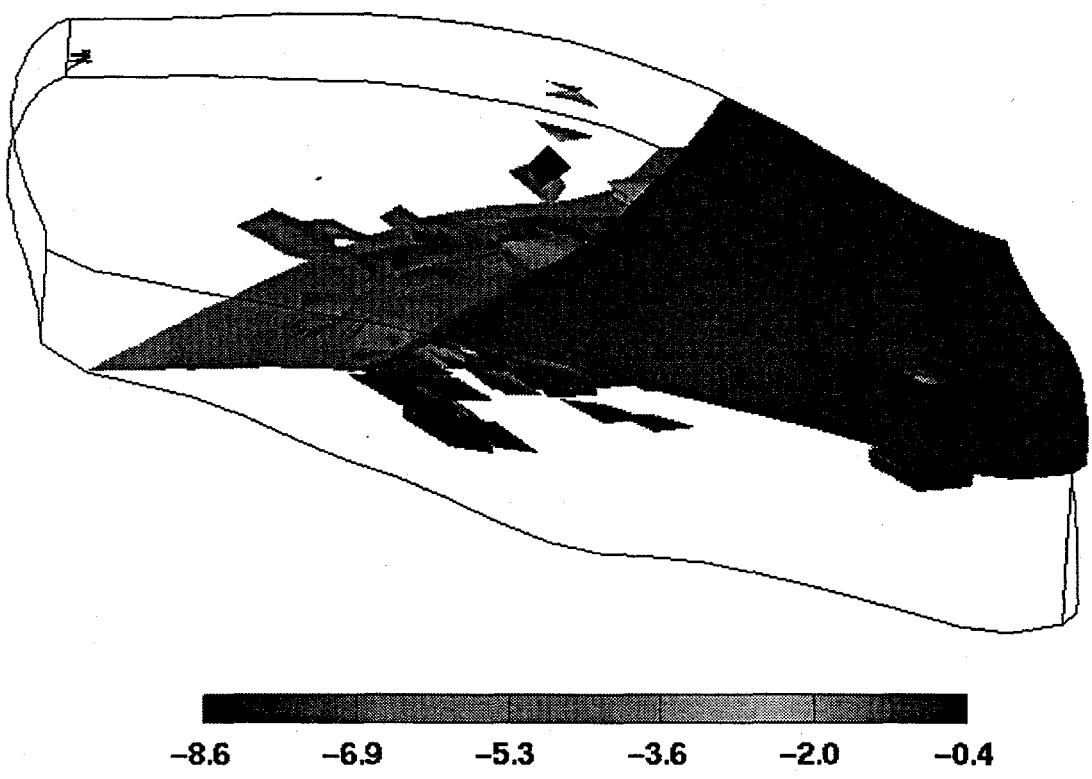

Fig. 6(b) Isosurface of 1 bar overpressure in the Anadarko Basin. Vertical exaggeration is 10x.

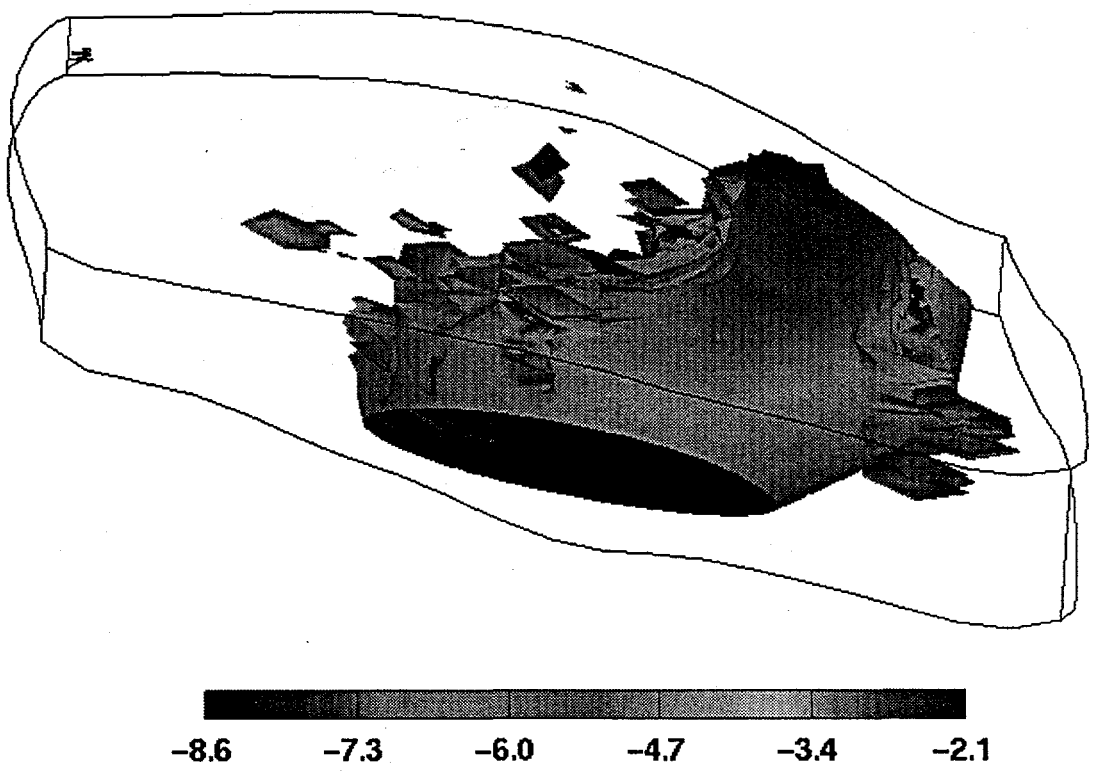

Fig. 6(c) Isosurface of 10 bars overpressure.

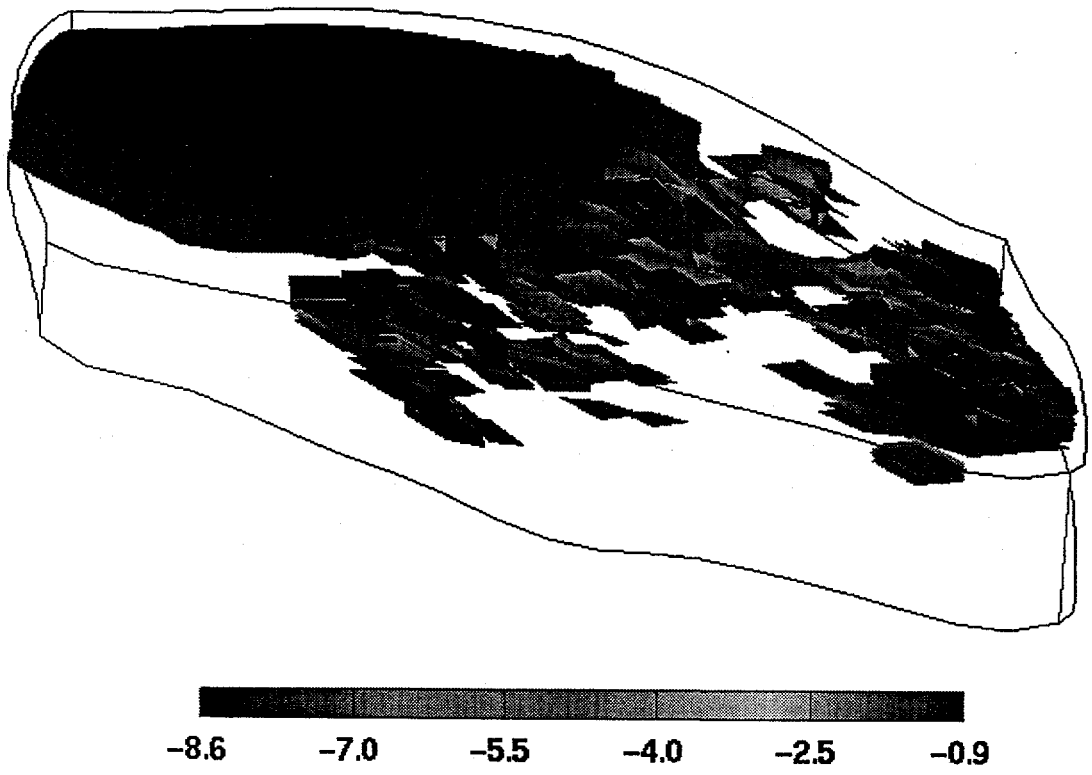

Fig. 6(d) Isosurface of 7 bars under pressure.

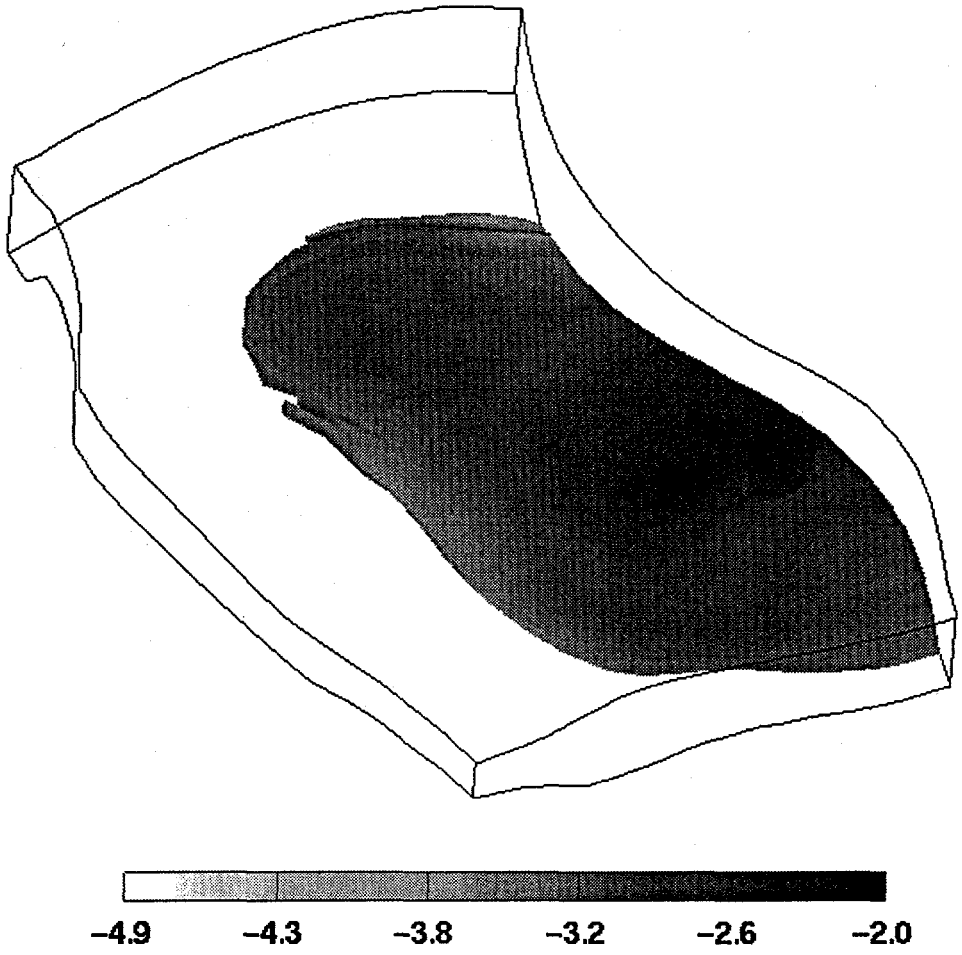

Fig. 7 Isosurface of 10 bars overpressure, using only the normal to overpressured data points of the highest quality data set.

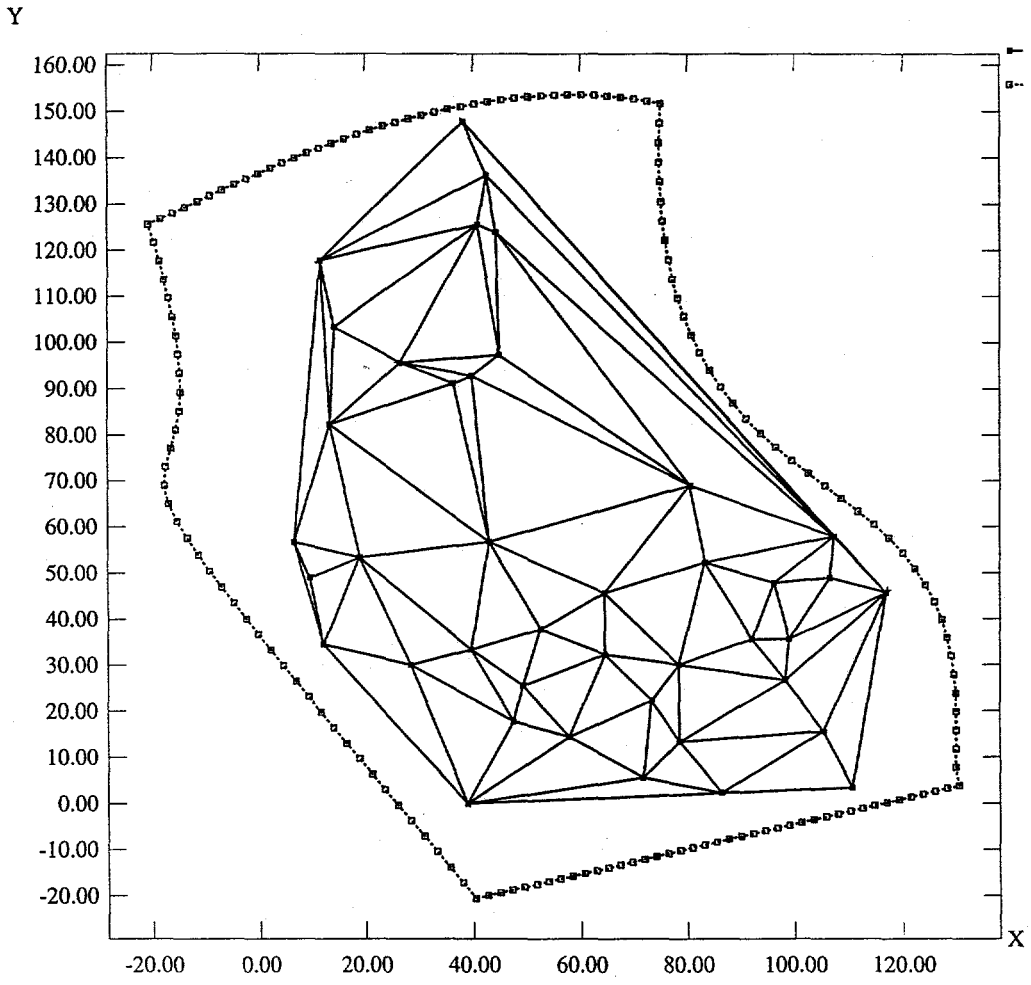

Fig. 8 Triangulation automatically created by our interpolation module that is part of our sedimentary history recreation module. Vertices of the triangles coincide with data well locations.

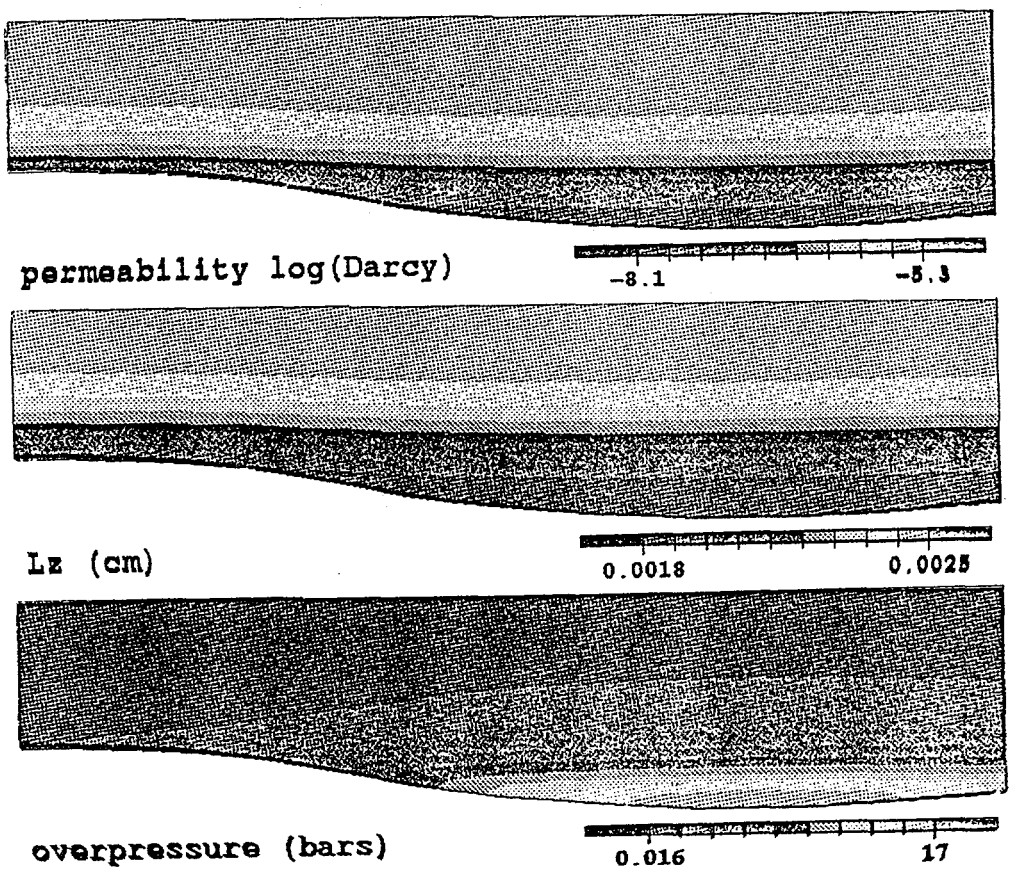

Fig. 9(a) Cross section through the three dimensional simulation domain at 50 my. Grain size is .0025 cm. No hydro-fractures have developed. Overpressuring is limited in extent and the maximum value is relatively low.

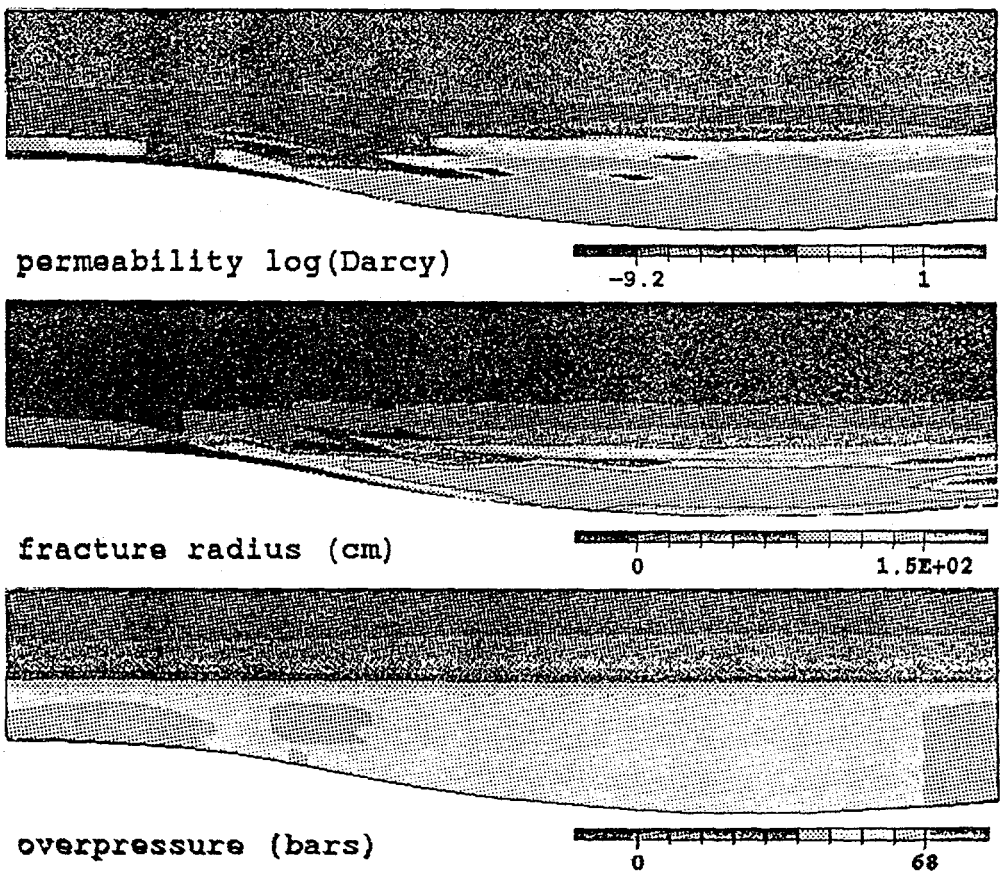

Fig. 9(b) Same as in Fig. 9(a), except that grain size is .001 cm. Hydro-fracturing has developed, and results in significant increase in permeability. A large overpressured compartment at the bottom of the basin is separated by a high pressure gradient zone. Pressure distribution in this compartment is patchy. The difference between case 9(a) and 9(b) illustrates the importance of developing an accurate sedimentary history for accurate fractured reservoir prediction.